Quaternary Science Reviews 321 (2023) 108346

Contents lists available at ScienceDirect

Quaternary Science Reviews

journal homepage: www.elsevier.com/locate/quascirev

Southern limit of the Patagonian Ice Sheet

Dominic A. Hodgson [a,*], Stephen J. Roberts [a], Eñaut Izagirre [b], Bianca B. Perren [a], François De Vleeschouwer [c], Sarah J. Davies [d], Thomas Bishop [e], Robert D. McCulloch [f,g], Juan-Carlos Aravena [h,i]

[a] British Antarctic Survey, High Cross, Madingley Road, Cambridge, CB3 0ET, UK
[b] Department of Geography, Prehistory and Archaeology, University of the Basque Country UPV/EHU, Vitoria-Gasteiz, Spain
[c] Instituto Franco-Argentino para el Estudio del Clima y sus Impactos, (CNRS-IRD-CONICET-UBA), Dpto. de Ciencias de la Atmosfera y los Oceanos, FCEN, Universidad de Buenos Aires, Argentina
[d] Geography and Earth Sciences, Llandinam Building, Penglais Campus, Aberystwyth University, SY23 3DB, UK
[e] Department of Geography, Arthur Lewis Building, Oxford Road, Manchester M13 9PL, UK
[f] Centro de Investigación en Ecosistemas de la Patagonia, Coyhaique, Aysén, Chile
[g] School of GeoSciences, The University of Edinburgh, Edinburgh, EH8 9XP, UK
[h] Centro de Investigación Gaia Antártica, Universidad de Magallanes, Punta Arenas, Chile
[i] Cape Horn International Center (CHIC), Puerto Williams 6350000, Chile

ARTICLE INFO

Handling Editor: Dr. C. O'Cofaigh

Keywords:
Quaternary
Glaciation
South America
Patagonia
Geomorphology
Last Glacial Maximum

ABSTRACT

The southern limit of the Patagonian Ice Sheet at glacial maxima is poorly constrained due to a paucity of field data. This particularly applies to southern outlet glaciers of the Cordillera Darwin whose full extents have been debated by glacial geologists since 1899 CE, introducing uncertainty into estimates of total ice volume. Here we report on the stratigraphy of exposed stratigraphic sections on the west coast of Isla Hermite which include glacial diamict with discontinuous boulder pavement, overlain by successions of peats and sandy silt. The location of these sections, orientation of clasts within the glacial diamict, and geomorphology of the adjacent marine trough, suggest that an ice stream extended south from an ice centre at Cordillera Darwin across an extended Magellan outwash plain, through Paso Mantellero, to Islas Hermite and Cabo de Hornos (Cape Horn). This was similar in extent to the Canal Beagle and Lago Fagnano Ice Lobes which extended to the east. Retreat occurred sometime before 12,880 cal yr BP based on radiocarbon dated peat macrofossils immediately overlying the glacial diamict. We discuss whether this is a close minimum age, or a product of delayed onset of peat accumulation at the sampling site.

1. Introduction

The configuration of the Patagonian Ice Sheet at glacial maxima has been extensively mapped from moraines, trimlines, drift deposits and other terrestrial and offshore glacial geomorphology. These data, accumulated over more than 190 years since Charles Darwin's visit on HMS Beagle (Darwin, 1846), have been refined with increasing methodological and chronological rigour as new techniques have become available. Notable advances include systematic descriptions of geomorphological deposits, widespread application of radiocarbon and other isotope dating methods to constrain the age of glacial features, and time slice reconstructions of whole ice sheet glaciation (see Davies et al., 2020 and references therein).

Despite these advances, there are still extensive regions where late Quaternary and Last Glacial Maximum (LGM) ice sheet extents remain poorly constrained, or where the geomorphological evidence is not reliably characterised or dated. For example, recent empirical reconstructions of the Patagonian Ice Sheet by Davies et al. (2020) identify the 'eastern Chilean Lake District, most outlet lobes in the Isla Grande de Chiloé sector, southcentral and western Patagonia through the archipelago and numerous outlet lobes of the Southern Patagonian Ice Field' as lacking geomorphological or chronological constraints on past ice extents. This lack of constraints limits confidence in reconstructions of past changes in regional ice mass that underpin models projecting future glacier responses to climate (Dussaillant et al., 2019). This is relevant because the Southern Andes are currently losing ice mass at a rate of

* Corresponding author.
E-mail address: daho@bas.ac.uk (D.A. Hodgson).

https://doi.org/10.1016/j.quascirev.2023.108346
Received 30 January 2023; Received in revised form 21 September 2023; Accepted 28 September 2023
Available online 25 October 2023

approximately 18.7 Gt yr^{-1} accounting for c. 7% of global glacier mass change 2000–2019 CE (Hugonnet et al., 2021).

At the southern limits of the Patagonian Ice Sheet, reconstructions of past ice extents originating from the ice centre at Cordillera Darwin (54.5°S, Fig. 1) have been inferred with 'low confidence' (red bounding lines; Fig. 1). This is because many of the ice lobes terminated offshore, are in difficult areas to access and study on land or because the geomorphological evidence has not been reliably characterised or dated. There are notable exceptions around the Estrecho de Magallanes, Bahía Inútil (Bentley et al., 2005; Darvill et al., 2015; Peltier et al., 2021), Lago Fagnano (Coronato et al., 2009; Waldmann et al., 2010) and Canal Beagle ice lobes where glacial geomorphological evidence (summarised in Fig. 2) underpins 'high' and 'medium confidence' assessments respectively (green and orange bounding lines; Fig. 1). Otherwise, most estimates of LGM and earlier limits in these areas rely on models (Hulton et al., 2002), and inferences of former glacial troughs from low resolution bathymetry, often on the basis of little direct evidence. This lack of evidence is most evident in the region south of the Canal Beagle (area delineated by red box in Fig. 2). As a result, there is a long history of conflicting interpretations of the southern limits of the Patagonian Ice Sheet in this region. These range from inferred LGM ice extents at or near the edge of the continental shelf in the earliest reconstructions by Nordenskjöld (1899), to LGM limits on the southern shore of Isla Navarino and through the middle of Isla Hoste around 55.20°South (Caldenius, 1932). This spatial uncertainty, and more recent interpretations of past ice extents are reviewed in Rabassa et al. (2011).

The southernmost lobe(s) of the last glacial ice sheet, that extended from an ice centre at Cordillera Darwin, remain particularly poorly constrained. Recent whole ice sheet GIS based landform assessments and General Bathymetric Chart of the Oceans (GEBCO) bathymetry infer the presence of an outlet glacier extending from the Cordillera Darwin, around Peninsula Dumas and Peninsula Hardy on Isla Hoste, towards the continental shelf break at 55–56°S with 'low confidence' (PATICE 35, 30 and 25 ka time slices in Fig; 1). However, there is no direct evidence of outlet glaciers occupying this region apart from unsupported inferences of ice extending south-south east across Isla Hoste (see Fig. 3 in Coronato et al., 1999). In this paper, we present evidence for an ice stream occupying Paso Mantellero, from stratigraphic sections and sediment cores on Isla Hermite, and from a reconstruction of the bathymetry of the adjacent marine trough. These suggest an ice stream extended south of Isla Navarino, through Bahía Nassau and along Paso Mantellero (between Isla Hoste and Isla Hermite) towards the edge of the continental shelf at 55.53°S. This marks the southern limit of the LGM Patagonian Ice Sheet.

1.1. Site description

Isla Hermite (55°51′S, 67°40′W, Fig. 2) is the westernmost of the Islas Hermite, which include Isla Hornos and Cabo de Hornos (Cape Horn). Isla Hermite is named after Jacques L'Hermite, who led the "Nassau Fleet," around Cabo de Hornos in 1624; its native Yaghan name is Samajani. The island is located at the southernmost limit of the South American continent, 100 km south of Puerto Williams (on Isla Navarino) and within the Cabo de Hornos National Park. It has a sub polar oceanic climate dominated by the Southern Hemisphere Westerly Winds, which have a local mean monthly intensity of 18.59–22.72 knots (34–42 km h^{-1}) and a maximum of 123 knots (228 km h^{-1}). Temperatures range from −1 to 13 °C, and the monthly mean relative humidities range from 85 to 89.6% (data from 40 km east of the sampling site at Cabo de Hornos Lighthouse; Centro Meteorológico Marítimo de Punta Arenas). The geology of the island comprises the Jurassic-Cenozoic intrusives and volcanic rocks characteristic of the south-western side of the Fuegian Andes (Torres Carbonell et al., 2016). The geomorphology of the eastern part of the island consists of rounded hills rising to c. 516 m, while the western part of the island has generally lower relief (30–100 m, reaching a maximum altitude of 427 m at Cerro West) (Fig. 3). The west coast of Isla Hermite consists of a series of small headlands, deeply incised inlets and coastal blowouts extending up to 500 m inland (Fig. 4), formed by direct exposure to Southern Ocean swells and the Southern Hemisphere Westerly Winds. The vegetation consists of Magellanic moorland including cushion plants, grasses, lichens and mosses, with extensive peat bogs and shallow peatland ponds at lower altitudes. Fragments of dwarf shrub heathland and stunted Magellanic subpolar forest trees including *Nothofagus antarctica* and *N. betuloides* persist inland and in protected valleys. Hill summits are largely devoid of higher vegetation but retain lichens and mosses (Fig. 3).

There are no published direct observations on the glacial geomorphology of Isla Hermite. Analysis of remotely sensed images has been used to infer five empty glacial cirques on the eastern (higher) parts of the island (shown on Fig. 2), and some potential glacial lineations oriented NNW to ESE were inferred from linear features on a promontory on the north east coast (Glasser and Jansson, 2008). The latter have not been ground-truthed or included in later compilations of the regional glacial geomorphology (Davies et al., 2020).

2. Methods

We carried out a geomorphological survey to identify evidence of glaciation on Isla Hermite, within a day's walk of a camp established on the north coast (research area delineated by the white box in Fig. 3). This included examining areas of bare rock for glacial striations, looking for glacial till and landforms associated with glacial transport such as erratic boulders, examining stratigraphic sections (SS) exposed by wind, fluvial or wave erosion, and sampling and describing the stratigraphy of sediment cores from peat bogs (PB), and shallow ponds (L).

Two stratigraphic sections were examined; one within and adjacent to coastal cliffs at Cabo West (SS2; 55.8438°S, 67.9091°W, ~30–45 m GPS altitude), and the other at Punta Momberg (SS1; 55.8295°S, 67.8991°W, ~14–20 m GPS altitude; Fig. 4). The sections were cleaned to reveal the succession of facies. Characterisation of the SS2 stratigraphic section at Cabo West included visual description of the lowermost unit (which could not be physically sampled as it was within an inaccessible cliff face at 55.8432°S, 67.9104 °W), direct sampling of mid units immediately above the cliff exposed by wind erosion, and sampling of upper units by coring through an overlying raised peat dome (HER42PB at 55.8433°S, 67.9095°W), and an adjacent peat depression with 20 cm surface water (HER42L at 55.8433°S, 67.9095°W; Fig. 4). Core sampling of other nearby shallow ponds was carried out to determine the onset of peat deposition and the spatial extent of the stratigraphic units exposed in the coastal sections (HER44L at 55.8442°S, 67.9072°W, 0.2 m deep; and HER49L at 55.8515°S, 67.9025°W, 0.5 m deep; Fig. 4). Studies of the SS1 stratigraphic section at Punta Momberg (Fig. 4) included duplicate sampling of the units exposed at Cabo West. A basic clast fabric analysis was also carried out on the lowermost unit by measuring the compass orientation of the long axes of elongate clasts. Core sampling of nearby peat depressions and shallow ponds was also carried out (HER14L at 55.8264°S, 67.8911°W, 0.4 m deep; HER24L at 55.8289°S, 67.8949°W, 0.5 m deep; HER34L at 55.8351°S, 67.9097°W, 0.5 m deep; Fig. 4).

Peat bogs, peat depressions with surface water and shallow ponds were sampled on foot (peat cores) or from a tethered boat (pond cores). Cores were retrieved using a 'Russian' peat corer (Belokopytov and Beresnevich, 1955) in 50 cm sections, from adjacent holes (20 cm apart), with a 10 cm overlap between each core section. Core sections were described, photographed, and transferred into 50 cm PVC half-pipe in the field, wrapped in cling film and layflat tubing, kept cool during transport to the UK, and then frozen and vacuum-packed for storage.

Cores were defrosted slowly while vacuum-packed to minimise shrinkage. To provide a basic description of the sedimentary facies. Non-destructive Geotek® multi-sensor core logging (MSCL) (Gunn and Best, 1998) was undertaken for gamma-ray wet density (ɣ-density; GRD), resistivity, magnetic susceptibility (MSκ; SIx 10^{-5}; Bartington

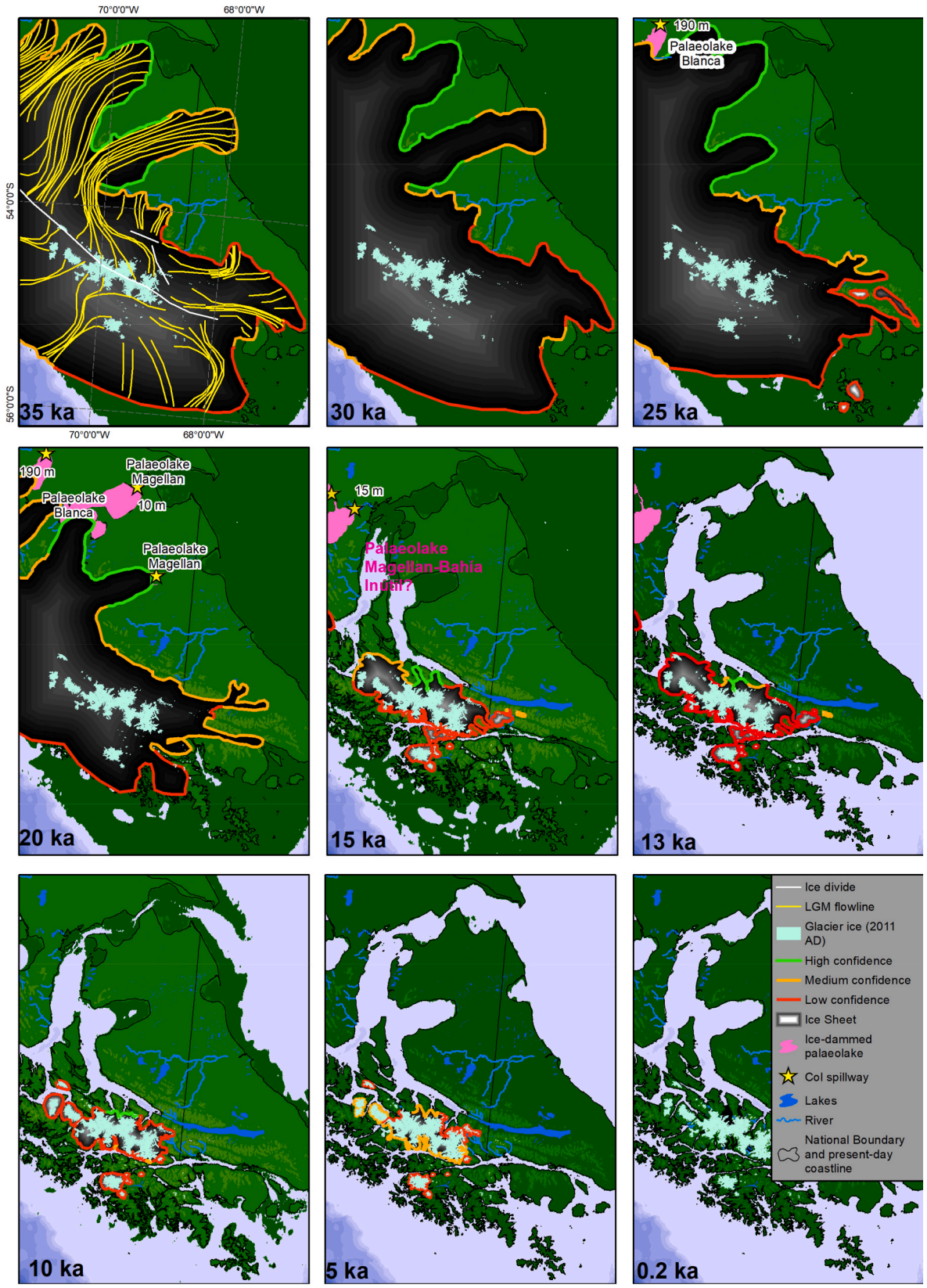

Fig. 1. Reproduction of Fig. 33 in Davies et al. (2020) showing reconstructions of the Patagonian Ice Sheet from an ice centre at Cordillera Darwin in time slices from 35 to 0.2 ka, together with General Bathymetric Chart of the Oceans (GEBCO) topographic and bathymetric data. Green shading marks the coastline during periods of lower relative sea levels based on data from Guilderson et al. (2000). Inferred ice-flow lines are shown in yellow for the 35 ka time slice.

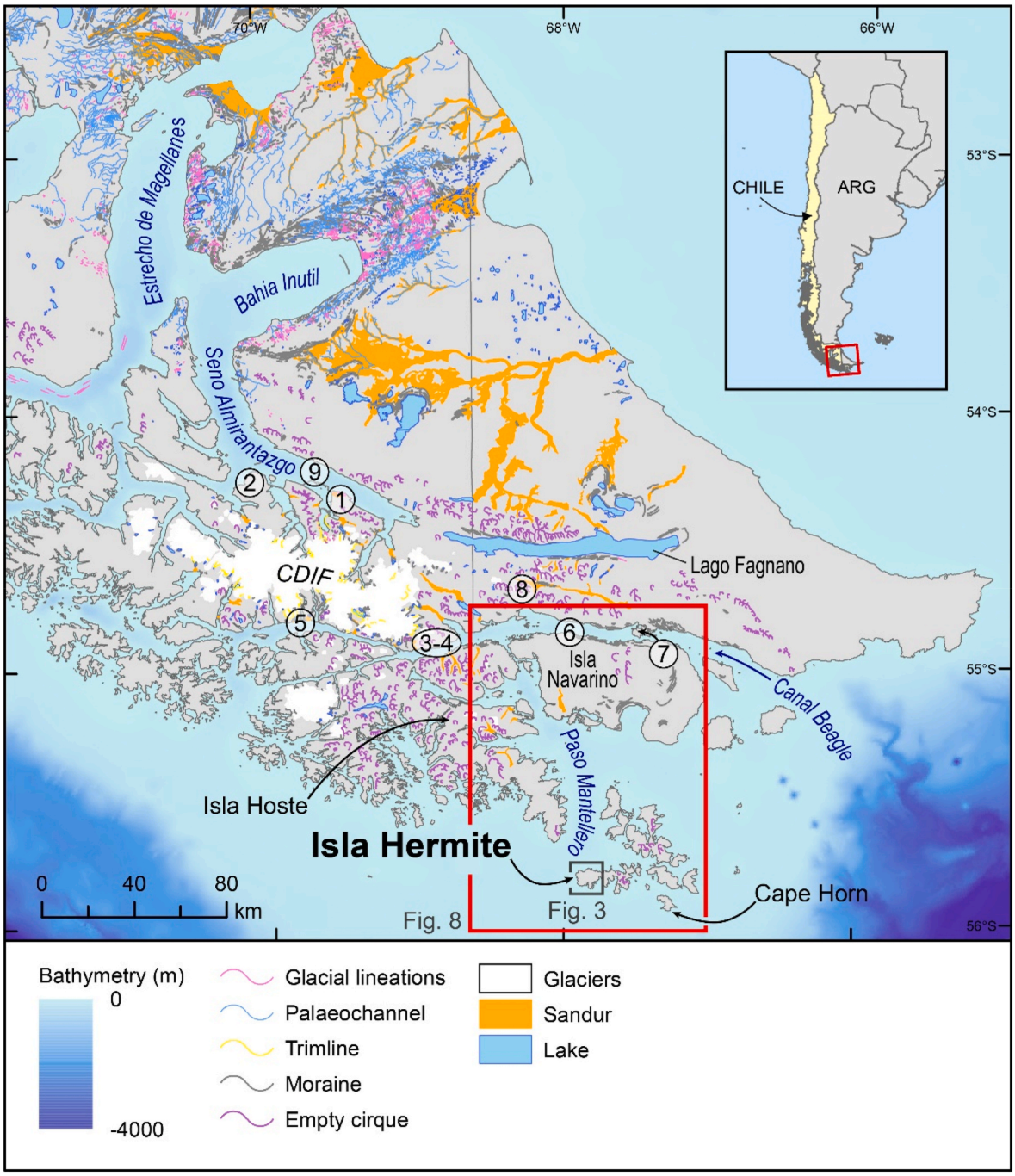

Fig. 2. Subset of PATICE (Davies et al., 2020) showing a regional overview of the glacial geomorphological features described across Tierra del Fuego derived from former Cordillera Darwin outlet glaciers. Locations cited in the text: 1 Punta Marinelli; 2 Punta Esperanza; 3 Caleta Olla; 4 Ventisquero Holanda; 5 Bahía Pía; 6 Punta Burslem; 7 Puerto Harberton; 8 Location of sites north of Ushuaia sampled by Menounos et al. (2013); 9 Location of sediment cores NBP0505-JPC67 and JPC77 in Seno Almirantazgo (Bertrand et al., 2017; Boyd et al., 2008); CDIF Cordillera Darwin Ice Field. The red box outlines the main study area South of Canal Beagle, and the small black box outlines the study area on Isla Hermite. Note the empty glacial cirques inferred on the eastern side of Isla Hermite.

Instruments: MS2E point sensor, 2 or 5 mm interval; 10 s measurement time) and volume specific (density-corrected) MSχ (κ/ρ; kg m^{-3}) data, and processed using Geotek Software (Gunn and Best, 1998). Digital X-radiographs were obtained using an ITRAX® X-ray fluorescence core scanner at Aberystwyth University. Core sections were aligned into composite records from field depth measurements, visual stratigraphy, digital X-radiographs, bulk density, MS, and XRF-CS scan data.

To provide chronological constraints, plant macrofossils from the top, bottom and main transitions within the stratigraphic sections, and in the lake sediment and peat cores were radiocarbon dated. Sediment and peat samples were acid washed; macrofossils underwent acid/alkali/acid pre-treatment. Radiocarbon analyses were performed at various labs (Beta Analytic USA, Keck-CCAMS Group USA, Scottish Universities Environmental Research Centre, and Laboratoire de Mesures du Carbone 14 in Paris). Calibration of radiocarbon ages was undertaken in OxCal v.4.4 (Bronk Ramsey, 2016) using the SHCal20.14C Southern Hemisphere atmosphere calibration dataset (Hogg et al., 2020). Bayesian age-depth models were constructed using BACON v.2.5 (Blaauw and Christen, 2011).

The bathymetry of Paso Mantellero and Bahía Nasau was

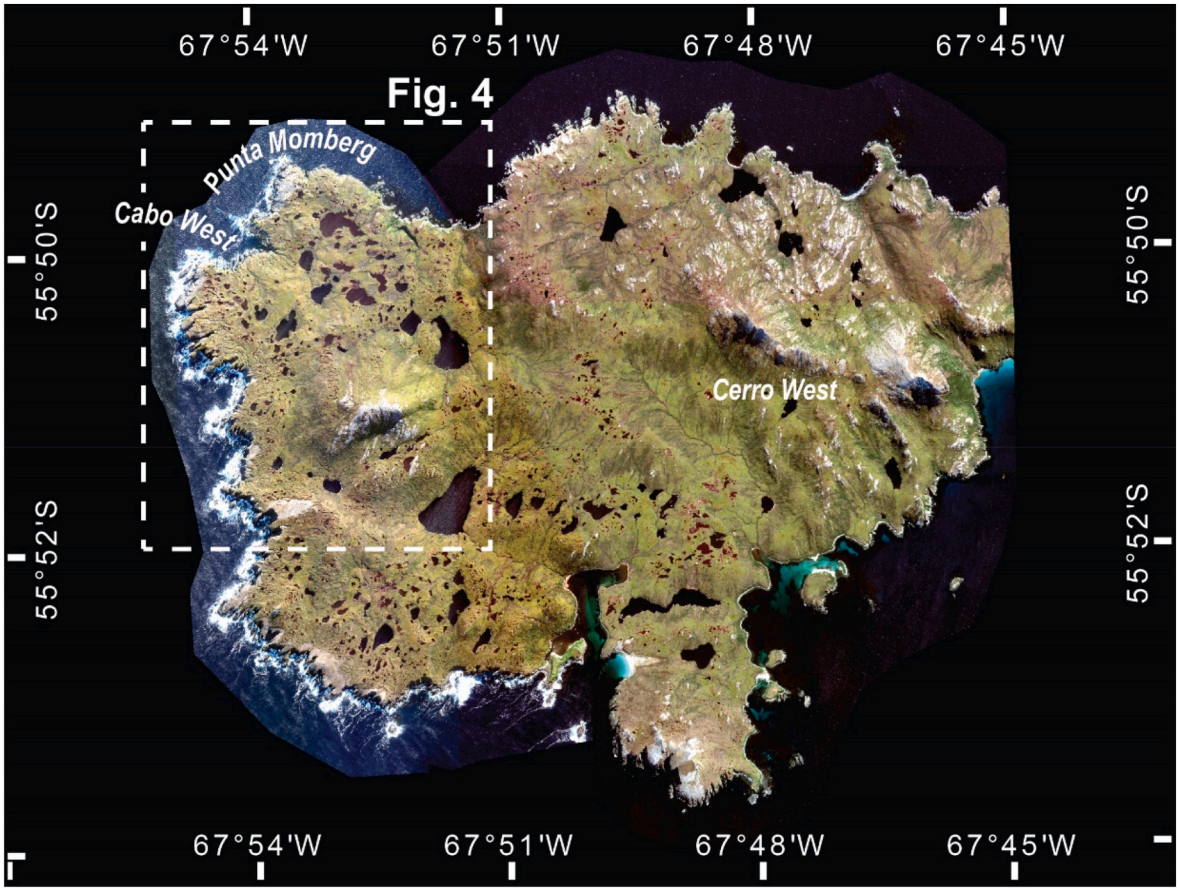

Fig. 3. Western part of Isla Hermite including Punta Momberg and Cabo West. White rectangle shows the location of the study area in Fig. 4. Image from Digital Globe WorldView-2, acquired April 28, 2012.

reconstructed from a combination of GEBCO gridded bathymetric data (https://www.gebco.net/) and hydrographic chart 'Islas Wollaston y Hermite por el Servicio Hidrográfico y Oceanográfico de la Armada de Chile' (Armada-de-Chile, 2000). Isobaths were interpolated at 10 and 50 m depth intervals.

3. Results

3.1. Glacial geomorphology

Evidence of glacial geomorphology was limited in the study area, except for basal units in the stratigraphic sections at Cabo West and Punta Momberg, described below. Three rock surfaces were found on upland areas which had linear erosion features (Supplementary Figs. 1B–D), but with different orientations aligned with local bedrock outcrops or weaknesses in the rock. Erratics were not present in the study area. All displaced boulders (e.g. Supplementary Fig. 1A) were derived from local bedrock rather than other Tierra del Fuego geologies. Inland peat exposures typically showed the accumulation of peat directly on bedrock or boulder-strewn bedrock surfaces (Supplementary Fig. 2) with maximum depths of peat exceeding 4 m.

3.2. Stratigraphic sections

Erosion of the cliffs on the west coast of Isla Hermite has exposed a sequence of late Quaternary deposits at Cabo West and Punta Momberg (SS2 and SS1; Fig. 4). These consist of four main stratigraphic units spread over a depth of ~10–14 m at Cabo West (Fig. 5), and ~ 2–4 m at Punta Momberg (Fig. 6).

Unit I, the basal unit, is in contact with the bedrock. Unit I is ~ 2–3 m thick where it is exposed in the cliff face at Cabo West (Fig. 5D) and ~ 1–2 m thick immediately inland of the cliff at Punta Momberg (Fig. 6C). It consists of a matrix supported clast moderate diamict (Dmm) including subangular to rounded boulders up to ~ 70 cm in length embedded within a sandy silty-clay matrix. Discontinuous horizontal layers of clasts, one particle thick, are evident both within the Unit (Fig. 5D) and on its upper limit (Fig. 5D and 6B) where it transitions to Unit II. These boulder pavements possibly mark former positions of the ice-till interface (cf. Benn and Evans, 2010, p. 383). Measurement of clast orientations in Unit I showed the long axes of most clasts were orientated between 330 and 0° (Fig. 6D). Further work on the geology of the clasts is required to determine their provenance.

At both sites, there is a sharp contact between Units I and II. Unit II consists of a dark brown desiccated peat with intact roots and woody plant fragments. Two macofossil radiocarbon ages on plant fragments immediately below and above the Unit I to Unit II contact at Punta Momberg (Fig. 6B) had median calibrated ages of 12,880 and 12,740 cal yr BP (radiocarbon dates 29 and 27 on Fig. 7A, and Supplementary Table 1). Bulk sediment ages were younger at 7760 and 10,320 cal yr BP respectively (radiocarbon dates 30 and 28 on Fig. 7A, and Supplementary Table 1), which we attribute to leaching of the humic acid fraction from the exposed face of the overlying peat (where it is subject to oxidation and high rainfall). At Cabo West the Unit I to Unit II transition could not be directly sampled for dating due to its inaccessible location in the cliff face. The age of the deepest accessible Unit II peat at Cabo West was 10,640 cal yr BP (radiocarbon date 54 on Fig. 7A, and Supplementary Table 1).

Unit III consists of layered grey-brown sands and silts. This 102 cm thick unit was deposited over a relatively short period of 640 years from 8650 to 8010 cal yr BP at Cabo West (Fig. 5C and 7A). An equivalent, but

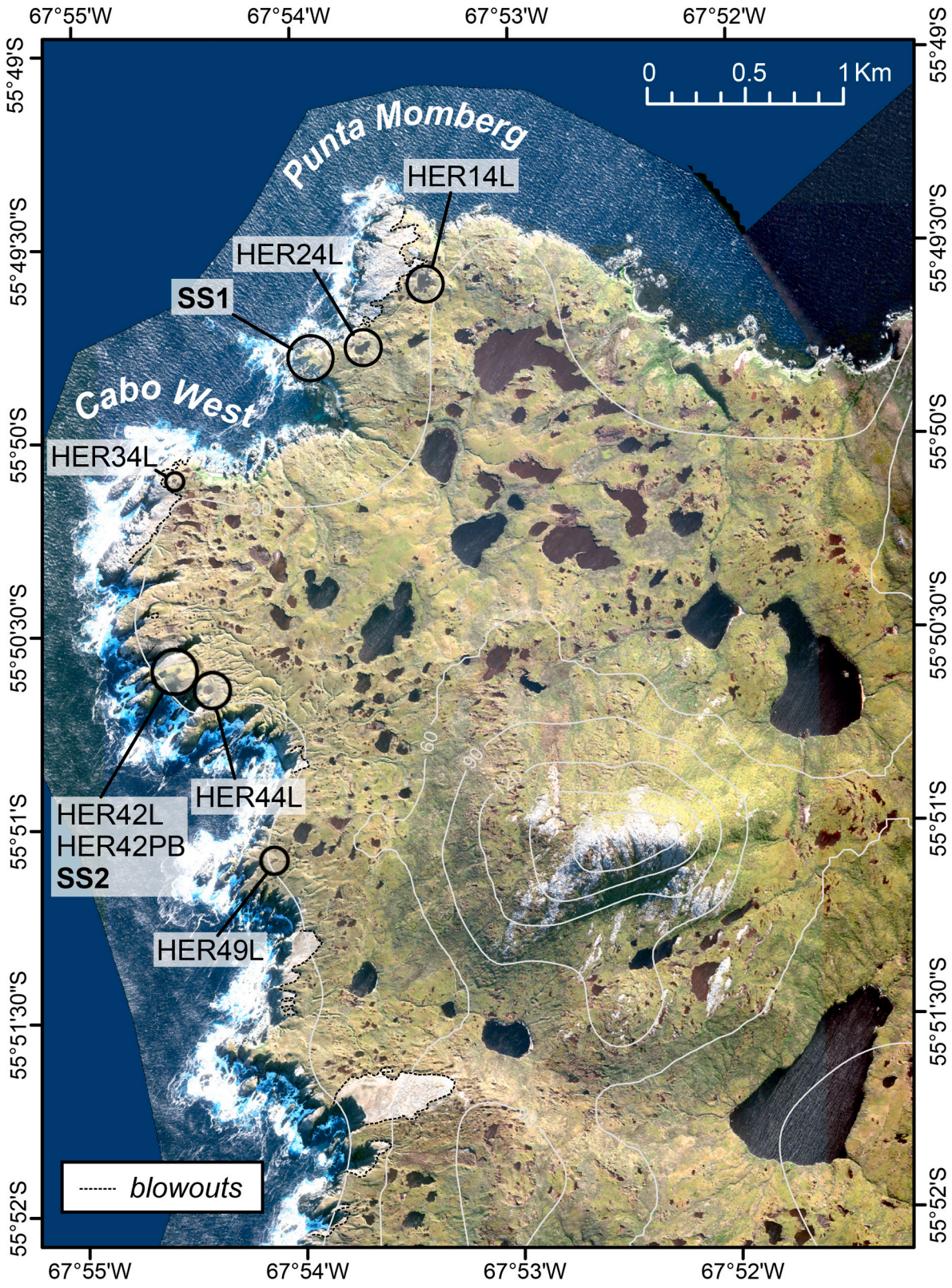

Fig. 4. West coast of Isla Hermite showing locations of the stratigraphic sections at Cabo West (SS2 and HER42PB) and Punta Momberg (SS1). Also shown are the locations of shallow lake cores (L) sampled at Cabo West (HER42PB, 42L, 44L, and 49L) and Punta Momberg (HER14L, 24L, and 34L). Dotted lines mark the locations of extensive coastal blowouts. Image from Digital Globe WorldView-2, acquired April 28, 2012.

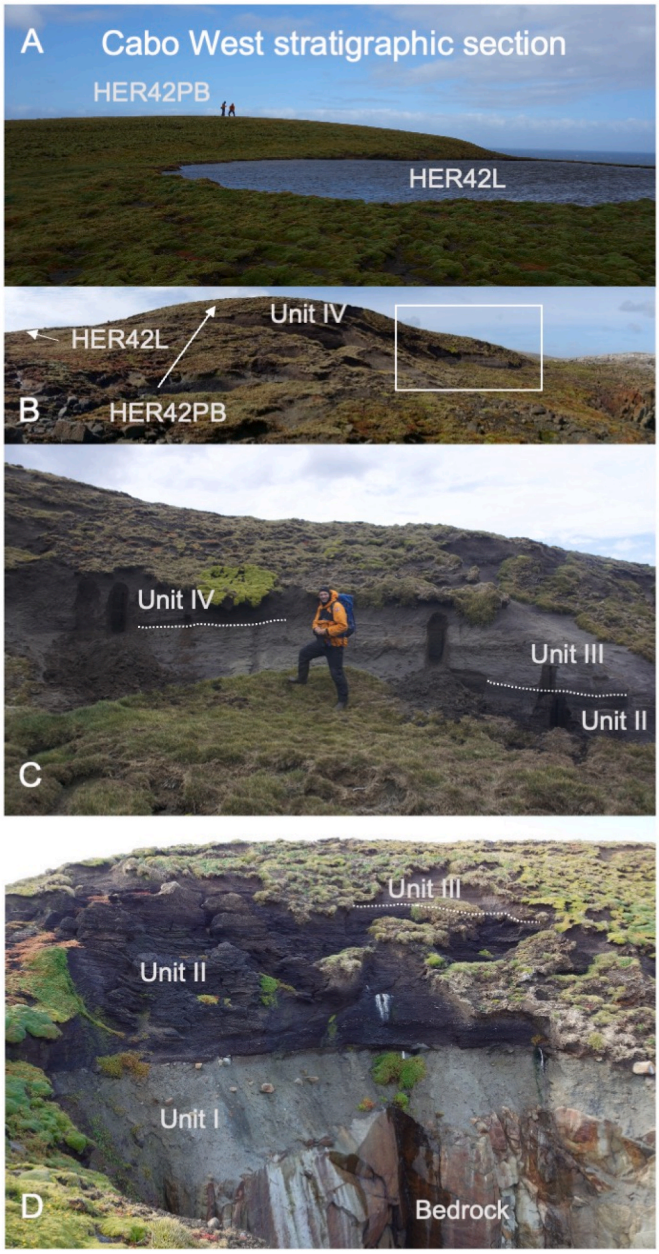

Fig. 5. Cabo West stratigraphic section (location SS2 in Fig. 4) showing photographs of the four lithological units overlying bedrock: Unit I Matrix supported clast moderate diamict, Unit II woody peat, Unit III sands and clays, Unit IV Holocene peat. A. Top of the section showing the domed peat bog (HER42PB) from which sediment cores were extracted to sample the upper parts of Unit IV and the adjacent shallow pond (HER42L) B. View of the deposits from the west coast showing the location of the exposed part of section and the location of panel C (white box). C. detail of the exposed section from which the lower parts of Unit IV, Unit III and the upper parts of Unit II were sampled. D. The base of the section as seen in the adjacent cliff face showing the underlying bedrock and Units I–III. The base of Unit II is inaccessible here without rope access, so samples for radiocarbon dating of the Unit I – Unit II transition were collected at the Punta Momberg stratigraphic section (Fig. 6B).

much thinner 3 cm layer was deposited around 8234 cal yr BP at Punta Momberg (Fig. 6B).

Unit IV consists of a relatively uniform Holocene peat with sand and grit layers, occasional clasts and fibrous plant remains. This was deposited from 8010 cal yr BP at Cabo West (Fig. 5B and C, Fig. 7A), and from sometime after 8230 cal yr BP at Punta Momberg (Fig. 6A and B). At Cabo West, radiocarbon dating shows that the lower part of Unit IV in

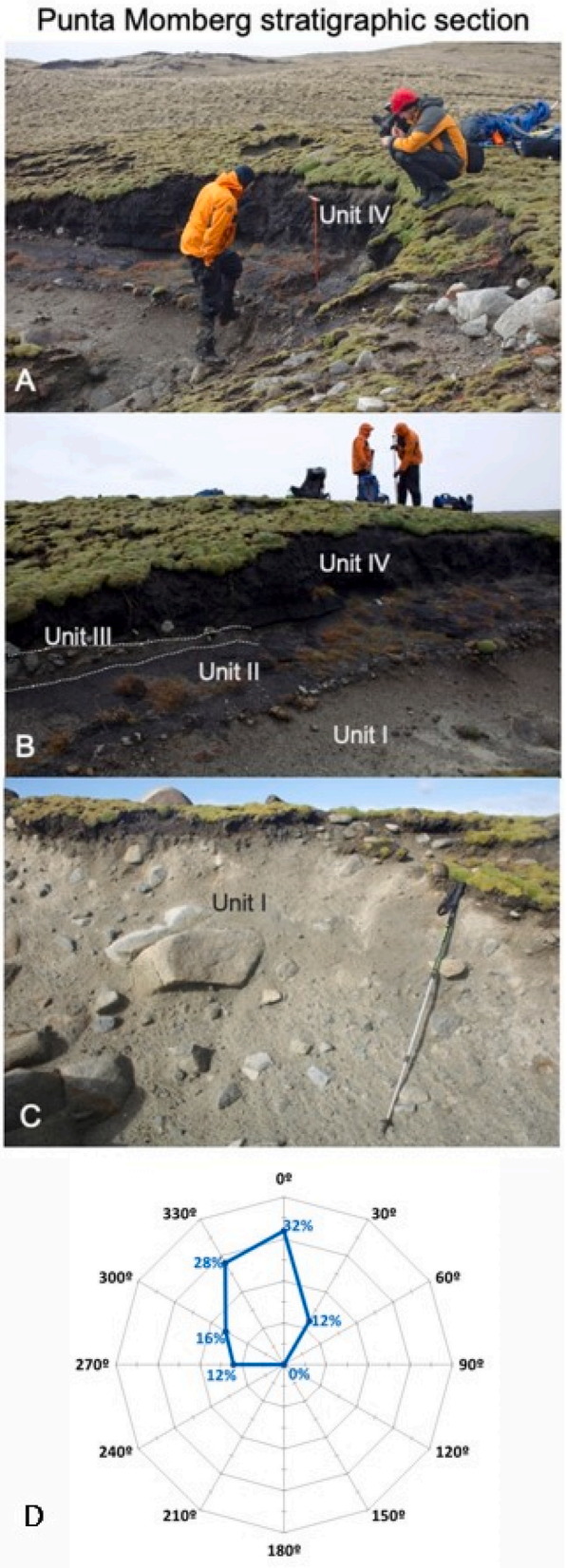

Fig. 6. Punta Momberg stratigraphic section (location SS1 on Fig. 4) showing photographs of the four lithological units. A. Overview of section. B. Detail showing Units I-IV. C. Detail showing Unit I with a walking pole for scale. D. Rose plot showing clast orientation in Unit I. The majority of clasts were orientated between 330 and 0° (n = 24), suggesting deposition by N–S flowing ice.

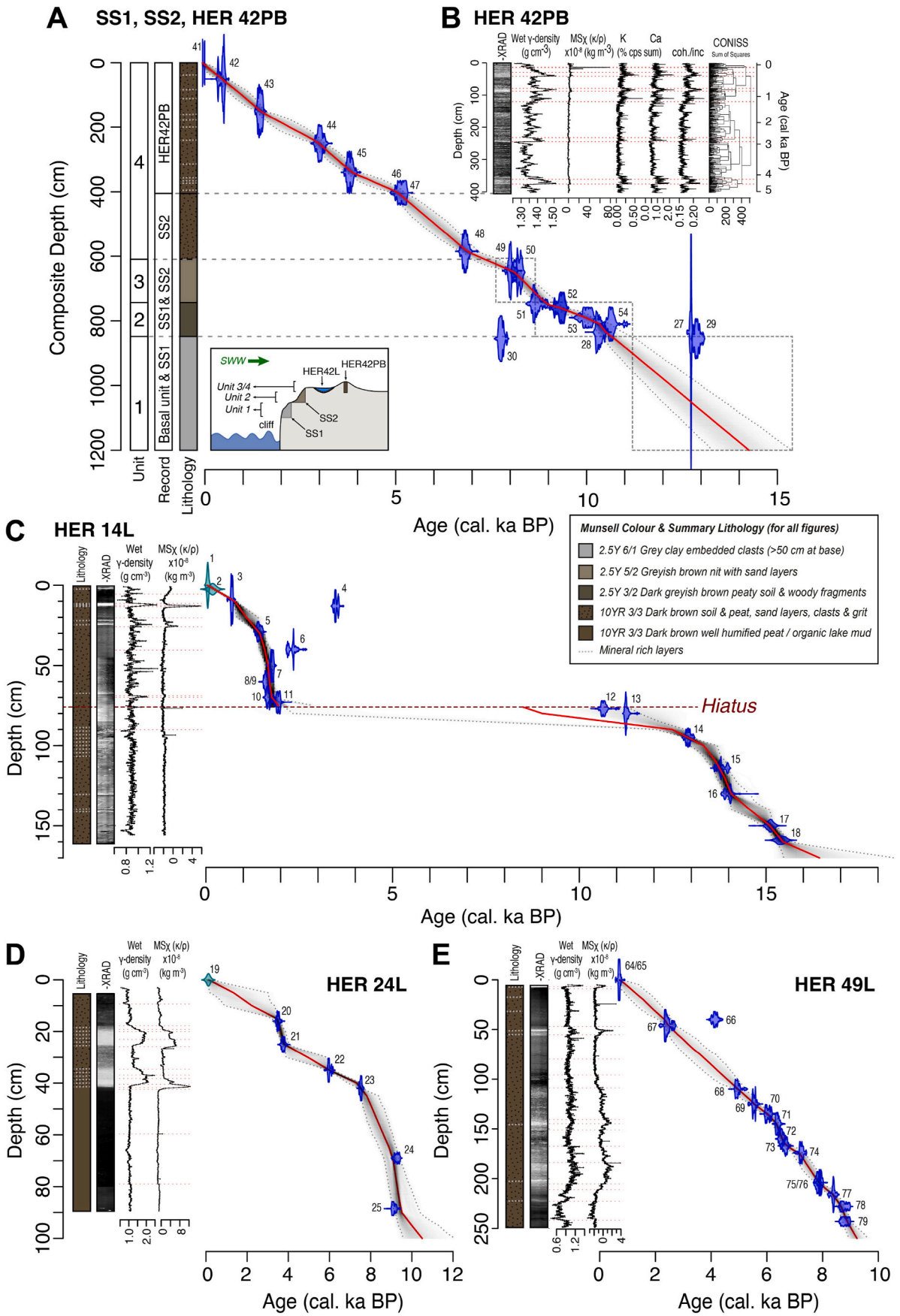

(caption on next page)

Fig. 7. A. Composite stratigraphic section from Cabo West including lithology and the age-depth model. The composite is based primarily on SS2, and the overlying HER42PB (Fig. 4). Inset box shows the relationship between the composite components. Radiocarbon ages for the base of Unit II were derived from Punta Momberg (SS1; Fig. 6B). B. X-ray image, wet density, magnetic susceptibility and selected XRF-CS measurements from the HER42PB peat core, which captures the upper 5160 cal yr BP of Unit I. C-E. Age-depth models including lithology, X-ray images, wet density and magnetic susceptibility data for selected shallow lake cores near Punta Momberg (HER14L, HER24L) and Cabo West (HER49L). Radiocarbon age ID numbers cross reference to data in Supplementary Table 1. We attribute the hiatus in HER14L to wind mixing causing remobilisation and deflation of the sediment, noting the large coastal blowout that currently extends to within 30 m of the lake shore (Fig. 4). These coastal blowouts can also erode into and capture the lakes, as seen elsewhere on the island (e.g., 55.8305°S, 67.8661°W). Note that the two peaks in wet density and magnetic susceptibility in HER 24L are interpreted as the product of tephra deposition.

the peat core (HER42PB) overlaps with the Unit IV peat sampled in the exposure (SS2) (Fig. 7A). The Unit IV peat in both the peat core (HER42PB) and adjacent peat depression (HER42L) have similar wet density, magnetic susceptibility and accumulation rates (0.089 and 0.075 cm yr^{-1} from the surface to 339 cm and 276 cm depths, respectively) (calculated from radiocarbon dates 41–45 and 34–40; Supplementary Table 1).

3.3. Sediment cores

Sediment cores from shallow lakes in the vicinity of the Cabo West stratigraphic section (HER44L, 0.15 km southeast of the section and 0.05 km inland; HER49L, 0.85 km south southeast and 0.1 km inland) had median basal ages of 8780 and 8800 cal yr BP (radiocarbon dates 62 and 79 in Supplementary Table 1). Measurements of wet density and magnetic susceptibility in HER 49L had values contiguous with the Unit IV peats in the Cabo West stratigraphic section (compare Fig. 7E–B). There is no evidence of Units I–III in HER44L (data not shown) and HER49L (Fig. 7E). Therefore, we assume the Unit IV peats at these locations accumulated on bedrock in the early to mid-Holocene.

Sediment cores from the shallow lakes in the vicinity of the Punta Momberg stratigraphic section (HER14L, 0.55 km northeast of the section and 0.32 km inland; HER24L, 0.2 km east and 0.2 km inland; and HER34L, 1 km southwest and 0.11 km inland) have median basal ages of 15,400, 9290 and 4300 cal yr BP respectively (radiocarbon ages 18, 24 and 33 in Supplementary Table 1). Measurements of wet density and magnetic susceptibility in HER14L and HER24L had values contiguous with the Unit IV peats in the Cabo West stratigraphic section (compare Fig. 7D, C and 7B). There is no evidence of Units I–III in HER14L, HER24L (Fig. 7C and D) and HER34 (data not shown). We therefore we assume that peat was accumulating on bedrock at these sites, immediately inland of the coast, from at least 15,400 cal yr BP.

3.4. Bathymetry of Paso Mantellero and Bahía Nassau

Paso Mantellero is a North-South trending submarine trough situated between Isla Hoste, Islas Wollaston and Islas Hermite (Fig. 8, Supplementary Fig. 3). Reconstructions of the bathymetry from hydrographic charts (Armada-de-Chile, 2000) and GEBCO data captured the large-scale morphology of the trough (Fig. 8). This revealed a broad valley landform characteristic of Patagonian land-terminating glacial land systems formed by ice advances during periods of lower (glacial) sea levels (Davies et al., 2020). Over-deepened basins between Peninsula Dumas and Isla Navarino, in Bahía Nassau and between Islas Wollaston and Isla Navarino may be the result of subglacial erosion through multiple glaciations. The shallow 40–80 m deep 'sills' between the basins may mark former moraines or ice limits as seen in other subantarctic fjords (Graham and Hodgson, 2014; Graham et al., 2017; Hodgson et al., 2014a).

4. Discussion

4.1. Absence of whole island glaciation

The absence of drift deposits and glacial geomorphology suggests the western Isla Hermite study area was not overridden during the last glaciation. If glacier ice was present, it likely only occupied the five inferred glacial cirques on the eastern uplands (Fig. 2 and Fig. 8). This limited local cirque glaciation is also implied from an inferred discrete ice mass on the eastern part of the island in the 25 ka time slice of the PATICE reconstruction (Fig. 1). A lack of consistency in the orientation of linear features observed on local bedrock surfaces suggests these are not glacial striations, but erosion of pre-existing weaknesses in the rock (Supplementary Figs. 1B–D). The absence of geologically distinct boulders, for example from the Lower Cretaceous plutonic and Devonian-Carboniferous metamorphic rocks that characterise the Cordillera Darwin (Sandoval and De Pascale, 2020), suggests there was no long-range transport of erratics onto the island. The rounded nature of the hills could be the result of earlier glacial activity but are more likely a product of intense salt and wind erosion; our measurements of specific conductivity in 57 surface water samples from lakes on the west of the island ranged from 0.3 to 7.1 mS cm^{-1} (Salinity 0.1 to 3.9 PSU) resulting from sea salt aerosol transport by winds which frequently reach gale force (28–55 knots). The dominance of the winds, in combination with the low altitudes, would have worked against in situ ice accumulation.

4.2. Ice stream occupying Paso Mantellero (before 12,880 cal yr BP)

We interpret the deposition of the Unit I glacial diamict, which is restricted to the western coastal stratigraphic sections at Cabo West and Punta Momberg, as being consistent with lateral moraine deposition by a c. 15–20 km wide ice stream extending c. 160 km from an ice centre at Cordillera Darwin and occupying Paso Mantellero during the Last Glacial (sometime before 12,880 cal yr BP) with bathymetry data suggesting it extended to 55.53°S (Fig. 8). The orientation of the clasts in Unit 1 (Fig. 6D) is indicative of a north to south ice flow direction of a topographically constrained ice stream, rather than radial deposition by a local island ice cap, or a coalesced ice cap across the Islas Hermite; which would have been a single landmass during periods of lower (glacial) relative sea level. Paso Mantellero reaches maximum depths of ~155 m below present sea level, so much of it would have been subaerially exposed as part of the extended Magellan outwash plain during the last glacial (Coronato et al., 1999), when relative sea levels have been modelled between −45 and −115 m at 20 ka (Björck et al., 2021; Guilderson et al., 2000, respectively). The altitude of the base of Unit I in the Cabo West and Punta Momberg sections above the deepest part of the trough provides a minimum constraint on ice stream thickness of c. 185–200 m.

An ice advance in Paso Mantellero has been inferred from ice flowlines in the 35 ka time slice in the PATICE model (Fig. 1; low confidence), and in 16 out of 21 gLGM PMIP model experiments with climate forcing (Fig. 13 in Yan et al., 2022). However, the timing of the Paso Mantellero ice retreat requires some consideration, as there is evidence both for and against 12,880 cal yr BP being a close minimum age for the Unit I to Unit II transition. This is discussed below.

4.2.1. 'Magellan Late Glacial advance hypothesis'

Our data provides a minimum age for ice stream retreat past Isla Hermite of 12,880 cal yr BP. The accumulation of peat shows that climatic conditions suitable for plant growth were established on the island from at least 15,400 cal yr BP (Her14L, Fig. 7C). This shows that there was a local source of plant propagules less than 550 m distance northeast of the Punta Momberg stratigraphic section, potentially allowing for a relatively rapid establishment of peat-forming plant communities on the

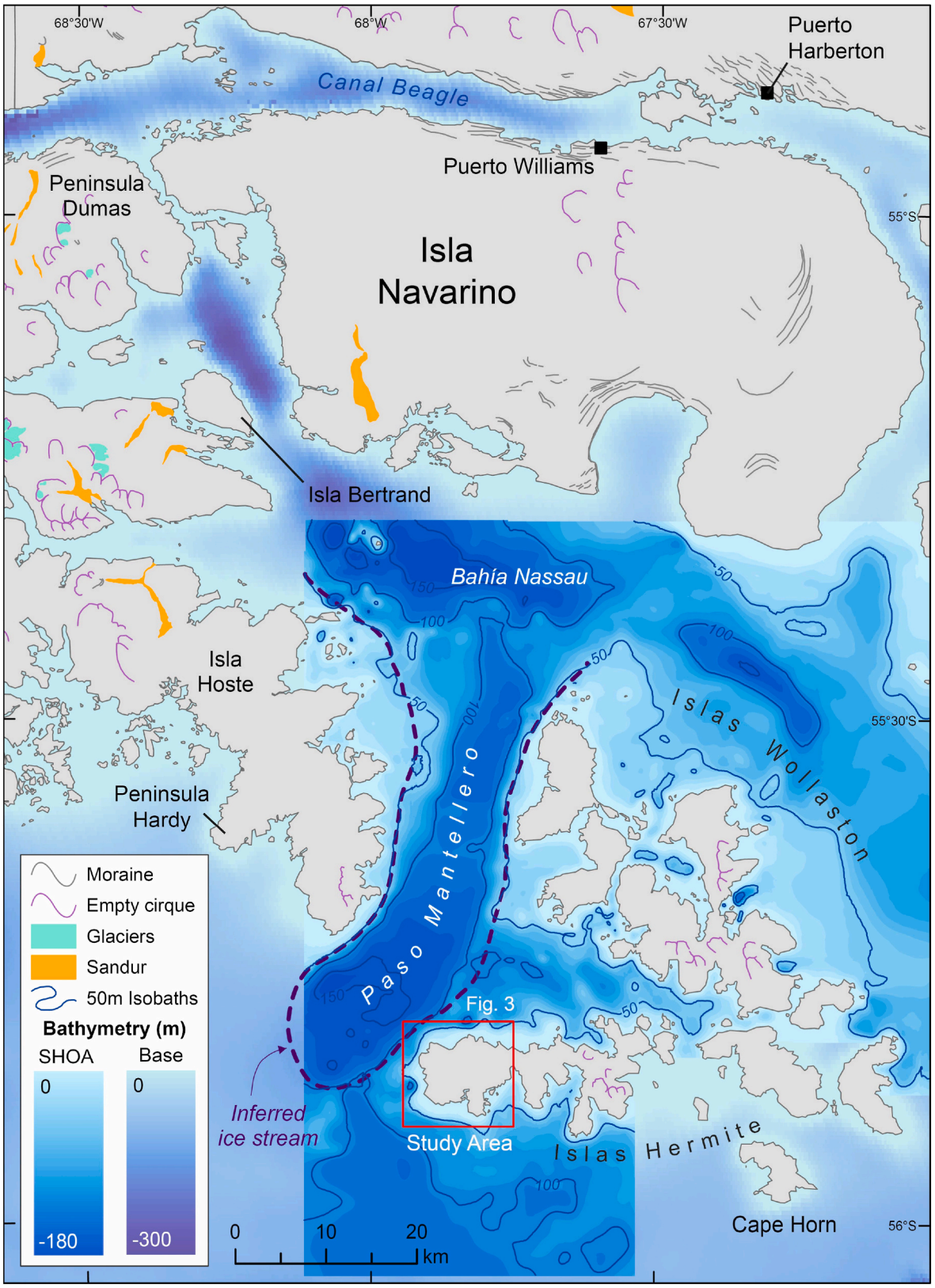

Fig. 8. Subset of PATICE (Davies et al., 2020) showing an overview of the terrestrial glacial geomorphological data in the region South of Canal Beagle together with a reconstruction of the bathymetry of Bahía Nassau and Paso Mantellero derived from GEBCO data (Base) and Servicio Hidrográfico y Oceanográfico de la Armada de Chile (SHOA) hydrographic charts (Armada-de-Chile, 2000). Dashed blue line shows the location of the 50 m isobath from which we infer the location, and southern limit, of the 'Paso Mantellero Ice Stream'.

Unit I glacial diamict following ice stream retreat. This might suggest that 12,880 cal yr BP is a close minimum age for retreat of ice following a Late Glacial ice advance. This 'Magellan Late Glacial advance hypothesis' requires contiguous proximity of the glacier ice with vegetated trough flanks, as observed in many Patagonian glaciers today.

Supporting evidence for Late Glacial ice advances in Patagonia include the 'Magellan Late Glacial advance' at 15,300–12,200 cal yr BP associated with the Antarctic Cold Reversal (Sugden et al., 2005), 'Glacial stage E' in the Estrecho de Magallanes (McCulloch et al., 2005b), cooler sea surface temperatures off the west coast of Chile at 41°S (Lamy et al., 2004) and similarly timed glacier advances in subantarctic South Georgia (Graham et al., 2017). This coincides with a maximum Antarctic Cold Reversal glacier extent in the Torres del Paine region (the TDP II moraines) at 14.2 ± 0.5 ka (mean ^{10}Be age) and glacier recession and deglaciation after 12,460 ± 70 cal yr BP (García et al., 2012). Evidence for advanced positions, or retreat from advanced ice positions, is also seen in some (but not all) of the Cordillera Darwin ice lobes around this time. For example, there is evidence of ice dammed lakes in the central Estrecho de Magallanes c. 17,000–12,250 cal yr BP (McCulloch et al., 2005a) with the last major advance of ice lobes into the southern Estrecho de Magallanes dated between c. 15,507–14,348 and 12,587–11,773 cal yr BP (McCulloch et al., 2005b). At the Lago Fagnano ice lobe (Fig. 2), onset of peat deposition from 'TSP San Pablo 1' east of Lago Fagnano commenced after 13,830–14,400 cal yr BP, and after 12,710–12,900 cal yr BP at 'LF Lago Fagnano' on the south east shore of the lake (Coronato et al., 2009). The C4 moraine was then formed by a grounded ice terminus located towards the western end of the lake at 11,170 cal yr BP; inferred from sedimentation rates below the H1 tephra dated at 7570 ± 120 cal yr BP (Waldmann et al., 2010); the age of the H1 tephra was subsequently revised by Stern et al. (2016) to 7891–8440 cal yr BP, based on radiocarbon dating of peat cores and lake sediments respectively.

If the 'Magellan Late Glacial advance hypothesis' is correct, retreat of the Paso Mantellero Ice Stream (following the advance) may have been driven by postglacial relative sea level rise, which flooded the Magellan outwash plain, converting the land terminating Paso Mantellero Ice Stream into a marine terminating glacier. This would have decreased the basal effective pressure of the ice stream increasing the calving rate and retreat of the calving front. Relative sea level reconstructions from nearby Canal Beagle, 110 km to the north (Fig. 8), show that postglacial relative sea level rise accelerated from 14,000 cal yr BP (Fig. 14 in Björck et al., 2021), exceeded present day sea level after c. 8600 cal, yr BP, and reached its maximum by c. 7000 cal yr BP (Figs. 9 and 14 in Björck et al., 2021) so we can assume flotation of the glacier terminus accelerated the retreat in the early Holocene. This interaction with relative sea level may, in part, explain differences between glacier responses in marine terminating ice lobes in the Magellan region compared with land terminating ice lobes of the Patagonian Ice Sheet at lower latitudes. Glacier responses to transitions from a marine-to terrestrially-based ice-sheet margins have also been described for the British–Irish Ice Sheet (Ó Cofaigh et al., 2021).

4.2.2. *'Early retreat hypothesis'*

In contrast to the 'Magellan Late Glacial advance hypothesis', a number of models and geochronological constraints suggest an earlier retreat of the Patagonian Ice Sheet in this region. For example, the modelled ice advance in Paso Mantellero inferred from PATICE LGM flowlines occurred from 35 to 30 ka ('low confidence', Fig. 1), and within the gLGM time slice in PMIP model experiments (Fig. 13 in Yan et al., 2022). The PATICE reconstruction shows that retreat of the Patagonian Ice Sheet from these maximum LGM extents commenced before 25 ka, reaching a configuration where ice lobes terminated in Lago Fagnano, Canal Beagle and Isla Bertrand ('medium confidence') and on Isla Hoste ('low confidence') by 20 ka (Fig. 1).

Geochronological data from the ice lobes that discharged into Seno Almirantazgo and East into Canal Beagle also suggest an earlier retreat history, with no evidence of a readvance during the Late Glacial or Antarctic Cold Reversal. For example, minimum ages from peat bogs suggest the eastern and central sectors of the Canal Beagle were ice free sometime before at 17,760 cal yr BP (Puerto Harberton, Figs. 2) and 17,040 cal yr BP (Punta Burslem, Fig. 2) (McCulloch et al., 2020), with the Puerto Harberton peat record showing dust accumulation from 16, 200 cal yr BP (Vanneste et al., 2015). At the southern end of the Fuegan Andes directly north of Ushuaia and Canal Beagle (Fig. 2), surface exposure ages (^{10}Be) from glaciated bedrock indicate that alpine areas were free of ice by c. 16.9 ka with subsequent ice advances limited to very local cirque glacier expansion (c. 2 km) at 14.83–12.85 ka (^{10}Be and ^{14}C ages) (Menounos et al., 2013). Similarly, peat bog basal ages at sites close to the present day Cordillera Darwin Ice Field suggest that ice retreated to the northern flank of Cordillera Darwin between 17,009 cal yr BP (Punta Marinelli, Figs. 2) and 16,356 cal yr BP (Punta Esperanza, Fig. 2) (Hall et al., 2013). Marine sediment core data from over deepened basins in Seno Almirantazgo show a transition from ice-proximal facies to ice-distal facies occurred in two steps: 'the first at c. 15,500 cal yr BP and the second at c. 12,500 cal yr BP marking the retreat of Marinelli Glacier from Seno Almirantazgo (core NBP0505_JPC77; Boyd et al., 2008), with marine fjord conditions established by 9800 cal yr BP (core NBP0505_JOC67; Bertrand et al., 2017). Basal dates of macrofossils from organic infills on the southern flank of the present-day Cordillera Darwin Ice Field include 12,097 cal yr BP (Caleta Olla, CO-07-02), 14,768 cal yr BP ('Ventisquero Holanda, H-07-01) and 10, 485 and 14,486 cal yr BP (Bahía Pía, BL-07-15 and BL-07-16 B; locations in Fig. 2) (Hall et al., 2013).

Overall, the geochronological evidence suggests, either different behaviors of the ice lobes originating from the ice centre at Cordillera Darwin ('Magellan Late Glacial advance' vs. 'early retreat' hypothesis'), or that many of the regional radiocarbon dates are not close minimum ages for ice retreat. The latter interpretation is consistent with the generally late onset of peat deposition at subantarctic latitudes. This has been attributed to the cold and dry conditions resulting from northward displacement of the sea ice and westerlies in the glacial delaying peat accumulation until climatic conditions favouring plant growth were established in the late glacial and early Holocene (see Table 1 in Hodgson et al., 2014b). We therefore cannot rule out that the ice advance occurred during MIS2 or earlier, as implied by the PATICE model (Fig. 1). The onset of woody peat accumulation (Unit II) overlying the diamict (Unit I) at Cabo West at 12,880 cal yr BP may therefore not be a close minimum age for the ice advance along Paso Mantellero.

5. Conclusions

This paper contributes to understanding the extent and volume of the Patagonian Ice Sheet during the last glacial. Glacial diamict deposited on the west coast of Isla Hermite suggest an ice stream, with a minimum thickness of c. 185–200 m, extended c. 160 km south from Cordillera Darwin down Paso Mantellero and past Isla Hermite to 55.53°S. This was larger than the Canal Beagle and Lago Fagnano Ice Lobes which extended c. 100 and 150 km to the east. It supports the interpretation that LGM ice extended to the Islas Hermite and Cabo de Hornos archipelagos, as first suggested by Nordenskjöld in 1899, and more recently inferred with 'low confidence' in the PATICE model by Davies et al. (2020; Fig. 1). Peat macrofossils at the Unit I to Unit II transition in stratigraphic sections provide a minimum age for retreat of the ice stream of 12,880 cal yr BP, but this is not considered a close minimum age due to the late onset of peat growth at high latitudes in the late glacial. Analyses of further terrestrial deposits and marine sediment cores are recommended to more fully constrain the history of this ice stream, together with swath bathymetry to identify landforms and bedforms associated with ice streaming, still stands, and lift off due to postglacial relative sea level rise (cf. Bertrand et al., 2017; Björck et al., 2021).

Author contributions

DAH and SJR wrote the grant supporting the work. DAH, SJR, EI and BP carried out the fieldwork which was coordinated by J-CA. SJR and DH carried out the stratigraphic and geochronological analyses and SJR, SJD and TB carried out MSCL and ITRAX analyses, with FDV providing the density correction and LMC14 radiocarbon dates. All authors contributed to the writing.

Declaration of competing interest

The authors declare that they have no known competing financial interests or personal relationships that could have appeared to influence the work reported in this paper.

Data availability

Data are deposited in the NERC Polar Data Centre under the citation: Hodgson, D.A., Roberts, S.J., (2023). Radiocarbon ages, geochemical and physical sedimentological data from stratigraphic sections, lake sediments and peat bogs from Isla Hermite, Chile, collected in 2015 [Data set]. NERC EDS UK Polar Data Centre.

Acknowledgements

Fieldwork was planned and facilitated by colleagues at Instituto Antártico Chileno (INACH) including José Retamales (Director), Dr Marcelo Leppe (Head of Scientific Department), Javier S. Arata (Collaborating scientist) Félix Bartsch, Wendy Rubio, Antonio Supanar (Head of Logistics and Science support), Universidad de Magallanes (J-C A, EI) and Ashly Fusiarski (BAS). The Armada de Chile is thanked for field input by the Captain and crews of icebreaker Almirante Óscar Viel, uplift by the Coastguard vessel CNS Alacalufe and permission to use hydrographic data. DAH, SJR and BBP were supported by NERC grant NE K004515 1. EI was supported by Fondecyt 1130381. J-CA was supported by Fondecyt 1130381 and ANID/BASAL FB210018. FDV was supported by a CNRS INSU-ARTEMIS grant for the AMS ^{14}C at the LMC14 Laboratory in Saclay, Paris. RMcC was supported by ANID R20F0002 (PATSER) and Fondecyt 1200727. Laura Gerrish and Bonnie-Claire Pickard (BAS) provided mapping expertise for Figs. 2 and 8. Steve Colwell (BAS), Paola Uribe Raibaudi (Dirección Meteorológica de Chile) and Felipe Rifo Esposito (Jefe Centro Meteorológico Marítimo Región de Magallanes y Antártica Chilena, Armada de Chile) are thanked for meteorological data from Cape Horn. The research was carried out under permits from Corporación Nacional Forestal Región de Magallanes y Antártica Chilena (334/2014) and Ministerio de Relaciones Exteriores Dirección de Fronteras y Límites del Estado (320/2014). We thank Bethan Davies and Sebastien Bertrand for their constructive reviews.

Appendix A. Supplementary data

Supplementary data to this article can be found online at https://doi.org/10.1016/j.quascirev.2023.108346.

References

Armada-de-Chile, 2000. Islas Wollaston y Hermite [material cartográfico] por el Servicio Hidrográfico y Oceanográfico de la Armada de Chile, Mapoteca. Disponible en Biblioteca Nacional Digital de Chile. http://www.bibliotecanacionaldigital.gob.cl/bnd/631/w3-article-331699. (Accessed 22 April 2022).

Belokopytov, I.E., Beresnevich, V.V., 1955. Giktorf's peat borers. Torfyanaya Promyshlennost' 8, 9–10.

Benn, D., Evans, D.J.A., 2010. Glaciers and Glaciation, second ed. Routledge.

Bentley, M., Sugden, D., Hulton, N.R.J., McCulloch, R., 2005. The landforms and pattern of deglaciation in the Strait of Magellan and Bahía Inútil, southernmost South America. Geogr. Ann. Phys. Geogr. 87, 313–333.

Bertrand, S., Lange, C.B., Pantoja, S., Hughen, K., Van Tornhout, E., Wellner, J.S., 2017. Postglacial fluctuations of Cordillera Darwin glaciers (southernmost Patagonia) reconstructed from Almirantazgo fjord sediments. Quat. Sci. Rev. 177, 265–275.

Björck, S., Lambeck, K., Möller, P., Waldmann, N., Bennike, O., Jiang, H., Li, D., Sandgren, P., Nielsen, A.B., Porter, C.T., 2021. Relative sea level changes and glacio-isostatic modelling in the Beagle Channel, Tierra del Fuego, Chile: glacial and tectonic implications. Quat. Sci. Rev. 251, 106657.

Blaauw, M., Christen, J.A., 2011. Flexible Paleoclimate Age-Depth Models Using an Autoregressive Gamma Process, pp. 457–474.

Boyd, B.L., Anderson, J.B., Wellner, J.S., Fernández, R.A., 2008. The sedimentary record of glacial retreat, Marinelli Fjord, Patagonia: regional correlations and climate ties. Mar. Geol. 255, 165–178.

Bronk Ramsey, C., 2016. OxCal 4, 4. https://c14.arch.ox.ac.uk/oxcalhtml.

Caldenius, C., 1932. Las glaciaciones cuaternarias de la Patagonia y Tierra del Fuego. Geogr. Ann. 14, 1–164.

Coronato, A., Salemme, M., Rabassa, J., 1999. Palaeoenvironmental conditions during th early peopling of southernmost south America (late glacial-early Holocene, 14-8 ka B.P.). Quat. Int. 53/54, 77–92.

Coronato, A., Seppälä, M., Ponce, J.F., Rabassa, J., 2009. Glacial geomorphology of the Pleistocene Lake Fagnano ice lobe, Tierra del Fuego, southern South America. Geomorphology 112, 67–81.

Darvill, C.M., Bentley, M.J., Stokes, C.R., Hein, A.S., Rodés, Á., 2015. Extensive MIS 3 glaciation in southernmost Patagonia revealed by cosmogenic nuclide dating of outwash sediments. Earth Planet Sci. Lett. 429, 157–169.

Darwin, C.R., 1846. Geological Observations on South America. Being the Third Part of the Geology of the Voyage of the Beagle, under the Command of Capt. Fitzroy, R.N. During the Years 1832 to 1836. Smith Elder and Co., London.

Davies, B.J., Darvill, C.M., Lovell, H., Bendle, J.M., Dowdeswell, J.A., Fabel, D., García, J.-L., Geiger, A., Glasser, N.F., Gheorghiu, D.M., Harrison, S., Hein, A.S., Kaplan, M.R., Martin, J.R.V., Mendelova, M., Palmer, A., Pelto, M., Rodés, Á., Sagredo, E.A., Smedley, R.K., Smellie, J.L., Thorndycraft, V.R., 2020. The evolution of the Patagonian Ice Sheet from 35 ka to the present day (PATICE). Earth Sci. Rev. 204, 103152.

Dussaillant, I., Berthier, E., Brun, F., Masiokas, M., Hugonnet, R., Favier, V., Rabatel, A., Pitte, P., Ruiz, L., 2019. Two decades of glacier mass loss along the Andes. Nat. Geosci. 12, 802–808.

García, J.L., Kaplan, M.R., Hall, B.L., Schaefer, J.M., Vega, R.M., Schwartz, R., Finkel, R., 2012. Glacier expansion in Southern Patagonia throughout the antarctic cold reversal. Geology 40, 859–862.

Glasser, N., Jansson, K., 2008. The glacial map of southern south America. J. Maps 4, 175–196.

Graham, A.G.C., Hodgson, D.A., 2014. Terminal Moraines in the Fjord Basins of Sub-antarctic South Georgia. Geological Society, London, Memoirs, London.

Graham, A.G.C., Kuhn, G., Meisel, O., Hillenbrand, C.-D., Hodgson, D.A., Ehrmann, W., Wacker, L., Wintersteller, P., dos Santos Ferreira, C., Römer, M., White, D., Bohrmann, G., 2017. Major advance of South Georgia glaciers during the Antarctic Cold Reversal following extensive sub-Antarctic glaciation. Nat. Commun. 8, 14798.

Guilderson, T.P., Burckle, L., Hemming, S., Peltier, W.R., 2000. Late Pleistocene sea level variations derived from the Argentine Shelf. G-cubed 1.

Gunn, D.E., Best, A.I., 1998. A new automated nondestructive system for high resolution multi-sensor core logging of open sediment cores. Geo Mar. Lett. 18, 70–77.

Hall, B.L., Porter, C.T., Denton, G.H., Lowell, T.V., Bromley, G.R.M., 2013. Extensive recession of Cordillera Darwin glaciers in southernmost south America during heinrich stadial 1. Quat. Sci. Rev. 62, 49–55.

Hodgson, D.A., Graham, A.G.C., Griffiths, H.J., Roberts, S.J., Ó Cofaigh, C., Bentley, M.J., Evans, D.J.A., 2014a. Glacial history of sub-Antarctic South Georgia based on the submarine geomorphology of its fjords. Quat. Sci. Rev. 89, 129–147.

Hodgson, D.A., Graham, A.G.C., Roberts, S.J., Bentley, M.J., Ó Cofaigh, C., Verleyen, E., Vyverman, W., Jomelli, V., Favier, V., Brunstein, D., Verfaillie, D., Colhoun, E.A., Saunders, K., Selkirk, P.M., Mackintosh, A., Hedding, D.W., Nel, W., Hall, K., McGlone, M.S., Van der Putten, N., Dickens, W.A., Smith, J.A., 2014b. Terrestrial and submarine evidence for the extent and timing of the Last Glacial Maximum and the onset of deglaciation on the maritime-Antarctic and sub-Antarctic islands. Quat. Sci. Rev. 100, 137–158.

Hogg, A.G., Heaton, T.J., Hua, Q., Palmer, J.G., Turney, C.S.M., Southon, J., Bayliss, A., Blackwell, P.G., Boswijk, G., Bronk Ramsey, C., Pearson, C., Petchey, F., Reimer, P., Reimer, R., Wacker, L., 2020. SHCal20 southern Hemisphere calibration, 0–55,000 Years cal BP. Radiocarbon 62, 759–778.

Hugonnet, R., McNabb, R., Berthier, E., Menounos, B., Nuth, C., Girod, L., Farinotti, D., Huss, M., Dussaillant, I., Brun, F., Kääb, A., 2021. Accelerated global glacier mass loss in the early twenty-first century. Nature 592, 726–731.

Hulton, N.R.J., Purves, R.S., McCulloch, R.D., Sugden, D.E., Bentley, M.J., 2002. The last glacial maximum and deglaciation in southern south America. Quat. Sci. Rev. 21, 233–241.

Lamy, F., Kaiser, J., Ninnemann, U., Hebbeln, D., Arz, H.W., Stoner, J., 2004. Antarctic timing of surface water changes off Chile and patagonian ice sheet response. Science 304, 1959–1962.

McCulloch, R.D., Bentley, M.J., Tipping, R.M., Clapperton, C.M., 2005a. Evidence for late-glacial ice dammed lakes in the central Strait of Magellan and Bahía Inútil, southernmost South America. Geogr. Ann. 87 A, 335–362.

McCulloch, R.D., Blaikie, J., Jacob, B., Mansilla, C.A., Morello, F., De Pol-Holz, R., San Román, M., Tisdall, E., Torres, J., 2020. Late glacial and Holocene climate variability, southernmost Patagonia. Quat. Sci. Rev. 229, 106131.

McCulloch, R.D., Fogwill, C.J., Sugden, D.E., Bentley, M.J., Kubik, P.W., 2005b. Chronology of the last glaciation in central strait of magellan and bahía inútil, southernmost south America. Geogr. Ann. Phys. Geogr. 87, 289–312.

Menounos, B., Clague, J.J., Osborn, G., Davis, P.T., Ponce, F., Goehring, B., Maurer, M., Rabassa, J., Coronato, A., Marr, R., 2013. Latest Pleistocene and Holocene glacier fluctuations in southernmost Tierra del Fuego, Argentina. Quat. Sci. Rev. 77, 70–79.
Nordenskjöld, O., 1899. Geolgie, Geographie und Anthropologie. Scwedischen Expedition nach den Magellansländern, 1895-1897. Norstedt & Söner, Stockholm.
Ó Cofaigh, C., Callard, S.L., Roberts, D.H., Chiverrell, R.C., Ballantyne, C.K., Evans, D.J. A., Saher, M., Van Landeghem, K.J.J., Smedley, R., Benetti, S., Burke, M., Clark, C.D., Duller, G.A.T., Fabel, D., Livingstone, S.J., Mccarron, S., Medialdea, A., Moreton, S. G., Sacchetti, F., 2021. Timing and pace of ice-sheet withdrawal across the marine–terrestrial transition west of Ireland during the last glaciation. J. Quat. Sci. 36, 805–832.
Peltier, C., Kaplan, M.R., Birkel, S.D., Soteres, R.L., Sagredo, E.A., Aravena, J.C., Araos, J., Moreno, P.I., Schwartz, R., Schaefer, J.M., 2021. The large MIS 4 and long MIS 2 glacier maxima on the southern tip of South America. Quat. Sci. Rev. 262, 106858.
Rabassa, J., Coronato, A., Martinez, O., 2011. Late Cenozoic glaciations in Patagonia and Tierra del Fuego: an updated review. Biol. J. Linn. Soc. 103, 316–335.
Sandoval, F., De Pascale, G., 2020. Slip rates along the narrow Magallanes fault system, Tierra del Fuego region, Patagonia. Sci. Rep. 10, 8180.
Stern, C., Moreno, P., Henríquez, W., Villa-Martínez, R., Sagredo, E., Aravena, J., de Pol-Holz, R., 2016. Holocene tephrochronology around Cochrane (~47° S), southern Chile. Andean Geol. 43, 1–19.
Sugden, D.E., Bentley, M.J., Fogwill, C.J., Hulton, N.R.J., McCulloch, R.D., Purves, R.S., 2005. Late-glacial glacier events in southernmost South America: a blend of 'northern' and 'southern' hemispheric climatic signals. Geogr. Ann. Phys. Geogr. 87, 273–288.
Torres Carbonell, P.J., Guzmán, C., Yagupsky, D., Dimieri, L.V., 2016. Tectonic models for the Patagonian orogenic curve (southernmost Andes): an appraisal based on analog experiments from the Fuegian thrust–fold belt. Tectonophysics 671, 76–94.
Vanneste, H., De Vleeschouwer, F., Martinez-Cortizas, A., von Scheffer, C., Piotrowska, N., Coronato, A., Le Roux, G., 2015. Late-glacial elevated dust deposition linked to westerly wind shifts in southern South America. Nature Scientific Reports 5, 11670. https://doi.org/10.1038/srep11670.
Waldmann, N., Ariztegui, D., Anselmetti, F.S., Coronato, A., Austin, J.A., 2010. Geophysical evidence of multiple glacier advances in Lago Fagnano (54°S), southernmost Patagonia. Quat. Sci. Rev. 29, 1188–1200.
Yan, Q., Wei, T., Zhang, Z., 2022. Modeling the climate sensitivity of Patagonian glaciers and their responses to climatic change during the global last glacial maximum. Quat. Sci. Rev. 288, 107582.